

# The effect of temporal variations in rainfall on scale dependency in runoff coefficients

John Wainwright

Department of Geography, King's College London, London, UK

Anthony J. Parsons

Department of Geography, Leicester University, Leicester, UK

Received 3 January 2001; revised 28 February 2002; accepted 28 February 2002; published 5 December 2002.

[1] A series of numerical experiments was carried out to test the hypothesis that temporal variability of rainfall intensity during a storm can cause the commonly observed decrease in runoff coefficients with increasing slope length. The results demonstrate significant effects over even relatively short slope lengths. Sensitivity analyses show that the scale dependency of measured runoff coefficients is most sensitive to the infiltration parameters of the slope. Furthermore, it is also sensitive to the slope angle and the friction factor of the surface, because these parameters control the depth of overland flow. These results suggest that the combination of time-varying rainfall intensity during an event and run-on infiltration can provide an alternative to spatial variation in infiltration as an explanation for the scale-dependency of runoff coefficients that has been observed in the field. Overland-flow models which simply use the mean rainfall intensity are also shown to underpredict the runoff quite dramatically. The results imply that a better understanding of the temporal variability of rainfall intensities is important in both understanding field measurements and developing robust models of overland flow. *INDEX TERMS:* 1854 Hydrology: Precipitation (3354); 1860 Hydrology: Runoff and streamflow; *KEYWORDS:* runoff coefficient, run-on infiltration, overland-flow model, scale dependency

**Citation:** Wainwright, J., and A. J. Parsons, The effect of temporal variations in rainfall on scale dependency in runoff coefficients, *Water Resour. Res.*, 38(12), 1271, doi:10.1029/2000WR000188, 2002.

## 1. Introduction

[2] Scale dependency in runoff, wherein the measured runoff coefficient decreases as size of area increases, has been observed in a number of runoff studies. Lal [1997] showed a decrease in runoff coefficient from 5.15% for 10-m-long plots, to 4.7% at 20 m, 2.95% at 30 m, 2.25% at 40 m, and 1.85% at 60 m on plots cultivated under a rotation of maize and cowpeas in Nigeria. Van de Giesen *et al.* [2000] found runoff coefficients of 29% to 46% on 1-m<sup>2</sup> plots, compared with 6% to 27% on 9.6-m<sup>2</sup> plots, with a ratio of runoff coefficients under the same vegetation cover and land use of 0.20–0.59 on cultivated rice fields in the Ivory Coast. Median runoff coefficients on a ponderosa pine hillslope in northern New Mexico decreased from 8.3% on a 30-m<sup>2</sup> plot to 7.8% on a 355-m<sup>2</sup> plot and 1.4% on a 485-m<sup>2</sup> plot [Wilcox *et al.*, 1997]. Yair and Kossovsky [2002], working at a site in Israel, report runoff coefficients varying from 30 to 70% for 1.5-m<sup>2</sup> plots, reducing to 20–25% on 36-m<sup>2</sup> plots, with a further reduction to 5% on a 200-m<sup>2</sup> plot. These results support those found in an earlier paper by Yair *et al.* [1980], who stated that generally runoff produced in the uppermost parts of 60- to 70-m-long slopes rarely reached the slope base. Perhaps because the phenomenon is expressed in spatial terms, it is typically explained as a

function of spatial variation in infiltration. If infiltration is spatially varied such that for any given rainfall rate some parts of the surface have infiltration-excess runoff whereas other parts have unsatisfied infiltration demand, run-on infiltration will occur to satisfy part of this demand [e.g., Hawkins, 1982]. Assuming that the variability in infiltration is spatially random, as size (and specifically length) of the runoff-producing area increases, so too will the proportion of the infiltration demand that is met. Explanations based on spatial variability in this way have been put forward, for example, by Sharma *et al.* [1980], Dubreuil [1985], Merzougi and Gifford [1987], Williams and Bonell [1988], and Wilcox *et al.* [1997] for field examples, and by Sivapalan and Wood [1986], Julien and Moglen [1990], Larsen *et al.* [1994], Merz and Bárdossy [1998], Zhu *et al.* [1999], Artan *et al.* [2000], and Van Loon and Keesman [2000] in modeling studies. A variant of this idea is that put forward by Dunne *et al.* [1991], who argued that as the length of the runoff-producing area increases, so does the depth of runoff. Consequently, in an area of significant microrelief, a greater proportion of the surface will be inundated so that there will be an increase in the total water lost to infiltration. Similarly, some authors have pointed to small-scale spatial variability of rainfall rates as being important [Faurès *et al.*, 1995].

[3] An alternative explanation that might account for scale dependency of runoff coefficients under natural rainfall is the effect of temporal variations in rainfall intensity. Natural rainfall exhibits considerable temporal variation in

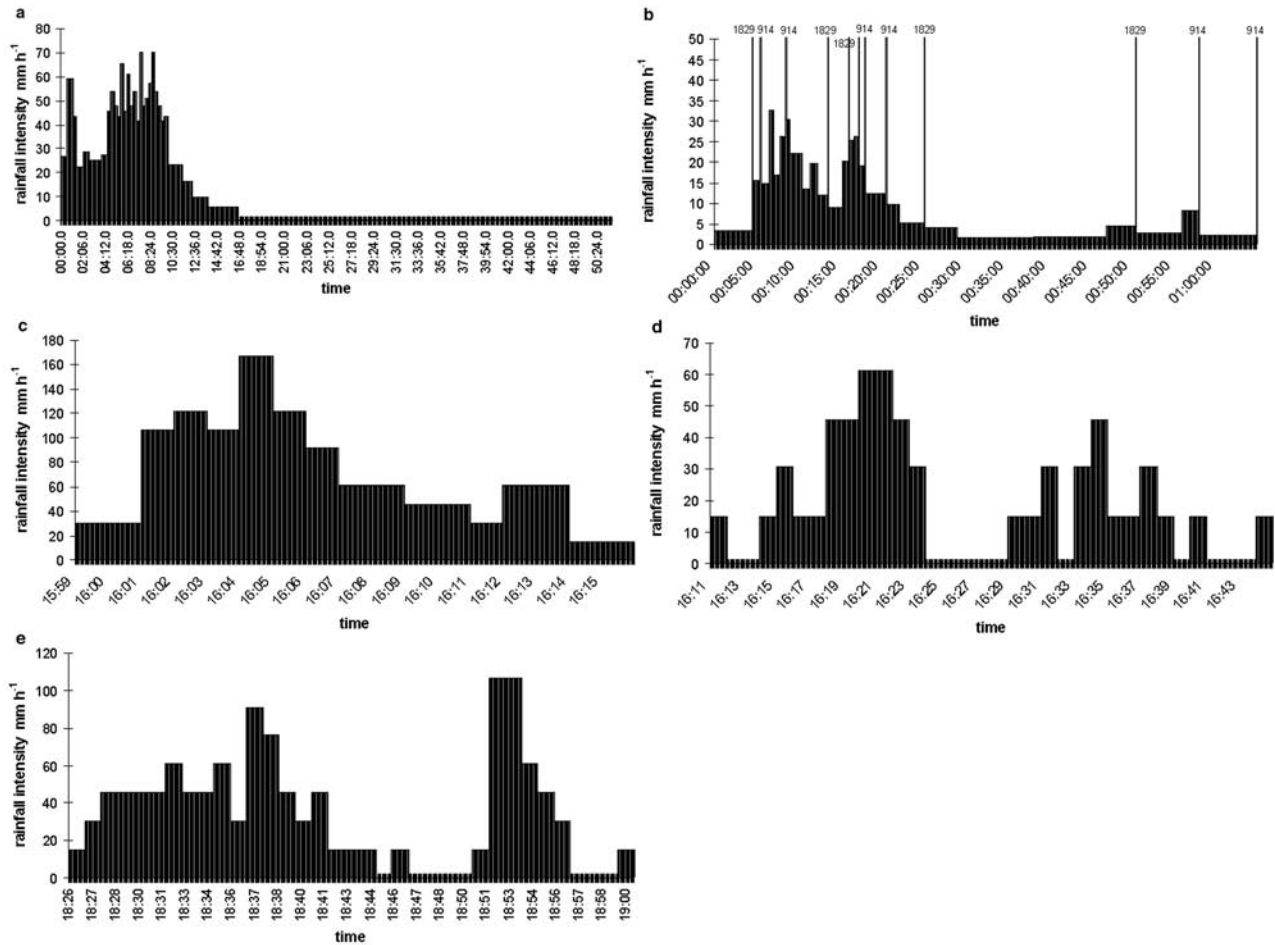


**Figure 1.** Rainfall hyetographs showing the great temporal variability in intensity observed during a single event.

intensity [Wainwright *et al.*, 1999] (Figure 1) so that even if the average rainfall intensity exceeds the infiltration rate for the soil, this might not be the case for some parts of the storm event. Pulses of runoff produced during parts of the storm could be lost to run-on infiltration during other parts of the storm when infiltration exceeded rainfall. These pulses would have a greater probability of being lost to run-on infiltration the farther downslope they travel. In consequence, as this paper will show, observed runoff coefficients will vary with runoff-producing area. This relationship is a natural extension of earlier studies that demonstrate a relationship with slope length as a function of the brief duration of storm events relative to the travel time taken for runoff produced at the top of the slope to reach its base [Yair *et al.*, 1980; Yair and Lavee, 1985; Van de Giesen *et al.*, 2000], and of modeling studies that demonstrate complex profile redistributions of water as a response to temporally variable rainfall [e.g., Corradini *et al.*, 1997].

## 2. Methods

[4] An overland-flow routing model is used to investigate the effects of temporal variability of rainfall inputs on runoff coefficients for differently sized plots. This cell-based model uses a simple infiltration model to generate overland flow, which is routed using the kinematic wave approximation

rated using the Darcy-Weisbach friction factor, with flow routing from cell to cell defined by the local topographic differences [Scoging *et al.*, 1992]. The model has been demonstrated to be effective in reproducing measured rates, hydraulics, and patterns of flow on semiarid hillslopes during constant-intensity rainfall-simulation events [Scoging *et al.*, 1992; Parsons *et al.*, 1997]. In the original form of the model, rainfall excess is calculated using a time-based approximation to the infiltration process that is dependent on only two parameters: the final infiltration rate after long time periods ( $a$ , in  $\text{mm h}^{-1}$ ) and the rate of change of infiltration under unsaturated conditions ( $b$ , in  $\text{mm}$ ). The parameters  $a$  and  $b$  are easily identifiable from rainfall-simulation experiments [see Abrahams and Parsons, 1991a; Scoging *et al.*, 1992; Parsons *et al.*, 1997], and the model provides a very good representation of infiltration under constant rainfall intensities in semiarid regions. At each model time step, the infiltration rate predicted from the infiltration equation is subtracted from the rainfall intensity, and the difference between the two rates (if positive) is assumed to be the amount of excess rainfall. However, this method of predicting infiltration cannot account for the process of run-on infiltration, which is central to the study undertaken here, or for time-varying rainfall rates, and so has been modified.

[5] To maintain the simplicity and ease of parameterization of the modified model, a single water-balance

**Table 1.** Summary Statistics of the Rainstorms Used in the Numerical Experiments

Storm Number	Location	Date, Time	Total Rain, mm	Range of Intensities, mm h <sup>-1</sup>	Average Intensity, mm h <sup>-1</sup>
1	Majuro	26/8/97, 1846–1938	8.3	0.4–70.3	9.6
2	Majuro	22/9/97, 0042–0147	10.0	1.6–1828.8	9.3
3	Jornada S watershed	30/7/97, 1559–1615	19.6	15–167.4	69.0
4	Jornada S watershed	20/7/98, 1611–1644	10.4	0–61.2	18.3
5	Jornada N watershed	14/8/97, 1826–1900	20.0	0–106.8	34.4

storage model has been used, following an approach similar to that of *Kirkby* [1978]. The infiltration equation used is

$$f = a' + \frac{s_{\max}}{s}, \quad (1)$$

where  $a' = a - 1$  [mm h<sup>-1</sup>] (allowing convergence to the final infiltration rate,  $a$ , at saturation, i.e., when  $s = s_{\max}$ ),  $s_{\max}$  is the total available soil-water storage [mm], and  $s$  is the current cumulated depth of water stored in the soil profile [mm]. The value of  $s_{\max}$  can be estimated from the same field data as  $a$  and  $b$  by taking the definite integral of equation (1) for the time taken to reach saturation (e.g., *Thornes and Gilman* [1984], who use a value of 1 hour). As the relationship is asymptotic, a fixed cutoff point needs to be used to produce consistent estimations once saturation has been reached. From the field data, saturation was always reached within a few minutes, and therefore truncation of the integral at 60 min will have minimal effect on the values produced, giving the relationship

$$s_{\max} = 4.094b. \quad (2)$$

Drainage from the base of the soil profile ( $p$ , mm h<sup>-1</sup>) was modeled using the empirical relationship

$$p = a \left( 1 - e^{b' [s_{\max}/s]} \right), \quad (3)$$

where  $b'$  (dimensionless) reflects the rate of convergence from unsaturated to saturated drainage conditions. For the simulations here, a constant value of  $b' = 5$  was used, which satisfactorily reproduced observed field rates, so that additional sources of variability were not introduced. Flow depth in each cell is calculated the kinematic wave assumption for flow routing, solved by a simple backward difference algorithm [*Scoging*, 1992]. Flow velocities are calculated using the Darcy-Weisbach friction factor, which can again be easily parameterized from field experiments [e.g., *Parsons et al.*, 1994].

[6] To allow run-on infiltration to be simulated, at each time step the depth of water on a cell is calculated as the existing flow depth plus the rainfall during the time step. Before runoff occurs, this value is simply the rainfall intensity. If the infiltration (from equation (1)) exceeds this value, then all the water on the surface is reinfilted, as well as the rain. If the infiltration is greater than the rainfall but less than the sum of the total water depth and the rainfall, then the difference is assumed to be the amount of run-on infiltration. Alternatively, if the infiltration is less than the current rainfall, no run-on infiltration is assumed to occur, and rainfall-excess runoff is generated as the difference between the rainfall and the infiltration. The current value of  $s$  is then calculated as the balance between its

previous value plus the current infiltration from rainfall and/or run-on, less the drainage from the base of the cell.

[7] A value of 8.6 mm h<sup>-1</sup> was chosen as the initial value for  $a'$ , which gives an equivalent final infiltration rate to the mean rainfall intensity of the first storm studied (and close to that of storm 2: see below for details), while the initial value of the  $s_{\max}$  parameter was 5.76 mm. The latter value was chosen as being the mean value for the experiments reported by *Parsons et al.* [1997], relating to soil conditions similar to those at the Jornada site, from which three of the studied storms are derived (see below).

[8] A total slope length of 500 m was employed, and the flow discharges at 1-m, 5-m, and then at 5-m intervals were used to calculate the runoff coefficients at points progressively down the slope. During the simulations, the time step was 0.5 s or 1 s, whichever was sufficient to maintain numerical stability, as confirmed by calculation of the Courant number. Total balance errors were of the order of 0.01%. In the simulations described here, a simple one-dimensional version of the model is used, with a cell size of 1 m × 1 m. Given that the size of these cells was relatively large in comparison to the mean flow velocities produced, tests were carried out to evaluate the potential effects of numerical diffusion on the results obtained. Root-mean-square errors ranged from 0.08% by comparison with a 0.10-m cell size, which is of an equivalent size for the kinematic wave to traverse during a single time step on average, to 0.12% at a 0.05-m cell size and 0.22% at a 0.01-m cell size. Therefore numerical diffusion was not considered to be an important problem for the time steps and cell sizes used.

[9] Two rainstorms were used from Majuro (Marshall Islands), based on data supplied from the National Oceanic and Atmospheric Administration (NOAA). These storms were used because intensity data were available at bucket-tip resolution, allowing demonstration of the large temporal variation in intensities. A further three rainstorms were selected from the Jornada Experimental Range in New Mexico [*Wainwright*, 2002]. These data were unfortunately only available as 1-min summaries, which is likely to lead to some underestimates in peak intensities. Summary statistics for each of the five storms used are presented in Table 1.

### 3. Results

[10] If the hypothesis is correct that temporal variation in rainfall intensity alone results in scale-dependent runoff coefficients, then such scale dependency will be manifest even when infiltration is both temporally and spatially uniform, provided that the infiltration rate is greater than the minimum rainfall intensity. Accordingly, in the first run of the model,  $s_{\max}$  was set to zero (to provide temporally uniform infiltration and prevent spatial variation due to the filling of the more downslope cells first) and all cells in the model had the same value of the final infiltration parameter

**Table 2.** Runoff Coefficients for Different Slope Lengths Using Infiltration Parameters  $a' = 8.6 \text{ mm h}^{-1}$ ,  $s_{\text{max}} = 0 \text{ mm}$ , and Friction Factor  $ff = 20$  Uniformly Distributed Along the Slope, on a  $5^\circ$  Slope Angle, for the Five Example Storms Outlined in Table 1

Slope Length, m	Runoff Coefficient, %				
	Storm 1	Storm 2	Storm 3	Storm 4	Storm 5
1	67.15	37.69	85.03	57.77	75.37
5	65.64	35.38	83.97	54.04	73.71
10	63.78	34.07	82.89	51.25	72.00
20	60.28	31.72	81.06	48.16	69.67
50	51.26	25.49	76.71	41.99	65.05
100	39.00	17.21	71.01	34.49	59.36
200	21.83	8.79	66.29	21.56	53.78
500	8.73	3.52	63.46	10.76	50.38

( $a' = 8.6 \text{ mm h}^{-1}$ ), to provide spatial uniformity. Results (Table 2) show that for the five storms, a significant decrease in the runoff coefficient occurs in all cases as slope length increases. This decrease does not occur when constant intensity rainfall is used.

[11] In a second series of simulations, the impact of temporal variability of rainfall was evaluated in a further series of numerical experiments using the initial values for  $a'$  and  $s_{\text{max}}$  to reflect conditions of spatial variability induced by the run-on-infiltration process. The runoff coefficient was found to decrease exponentially with increasing slope length in all cases (Table 3). The runoff coefficients for a 1-m slope for storms 1 and 2 were 13.4% and 0.8%, respectively, when the variable intensity rainfall was used, compared with 0% for equivalent constant intensity rainfall. For storm 3 the runoff coefficient was 35.9% for all slope lengths with constant intensity rainfall compared with 58.9% for a 1-m-long slope and 36.7% for a 500-m-long slope, using the variable rainfall. The other event with a high average intensity, storm 5, produced values of 24.3% for constant intensity rainfall compared with 48% (1-m slope) and 24.8% (500-m slope). Thus it can be seen that the use of constant intensity rainfall equivalent to the average intensity of the storm will produce underestimates of the runoff produced, whatever the slope length being simulated. The magnitude of this underestimate declines exponentially with slope length. These results demonstrate the importance of temporal variability in the rainfall input on the scale-dependency in runoff coefficients. The impact on predicted hydrographs can be seen by plotting the runoff per unit area at various points down the slope length (Figure 2). This measure illustrates the

**Table 3.** Runoff Coefficients for Different Slope Lengths Using Infiltration Parameters  $a' = 8.6 \text{ mm h}^{-1}$ ,  $s_{\text{max}} = 5.8 \text{ mm}$ , and Friction Factor  $ff = 20$  Uniformly Distributed Along the Slope, on a  $5^\circ$  Slope Angle, for the Five Example Storms Outlined in Table 1

Slope Length, m	Runoff Coefficient, %				
	Storm 1	Storm 2	Storm 3	Storm 4	Storm 5
1	13.44	0.81	58.91	8.84	47.98
5	11.65	0.18	57.81	7.12	46.70
10	9.73	0.09	56.67	5.59	45.57
20	6.55	0.05	54.78	3.55	43.69
50	2.70	0.02	50.38	1.45	39.32
100	1.35	0.01	44.65	0.72	33.75
200	0.68	$4.6 \times 10^{-3}$	39.71	0.36	28.20
500	0.27	$1.8 \times 10^{-3}$	36.73	0.14	24.81

progressive loss to run-on infiltration as the slope length increases.

[12] Given that spatial variations in infiltration rate are generally used to explain the downslope patterns in runoff coefficient, a further set of numerical experiments was carried out to explore the relative importance of this factor in comparison to the temporal variability in rainfall rates. These experiments were carried out by assessing the sensitivity to spatial variability in infiltration using three simple scenarios. In the first of these, the spatial variability was assumed to be random. Both the  $a'$  and  $s_{\text{max}}$  parameters were distributed using a normal distribution using the same values as described above for the mean parameter of the distribution, and with a standard deviation set to 10% of the mean value. The second scenario addressed the case of an infiltration rate generally increasing in a downslope direction. For simplicity, a linear trend was assumed, with values 10% greater at the base of the slope than at the top. A random component was incorporated by adding a normally distributed random number with a mean of zero and a standard deviation of 10% of the initial value. The third scenario was simply the reverse of the second, with the infiltration rate generally decreasing in a downslope direction.

[13] In all of the experiments, the level of the random variability imposed was insufficient to alter the general trends

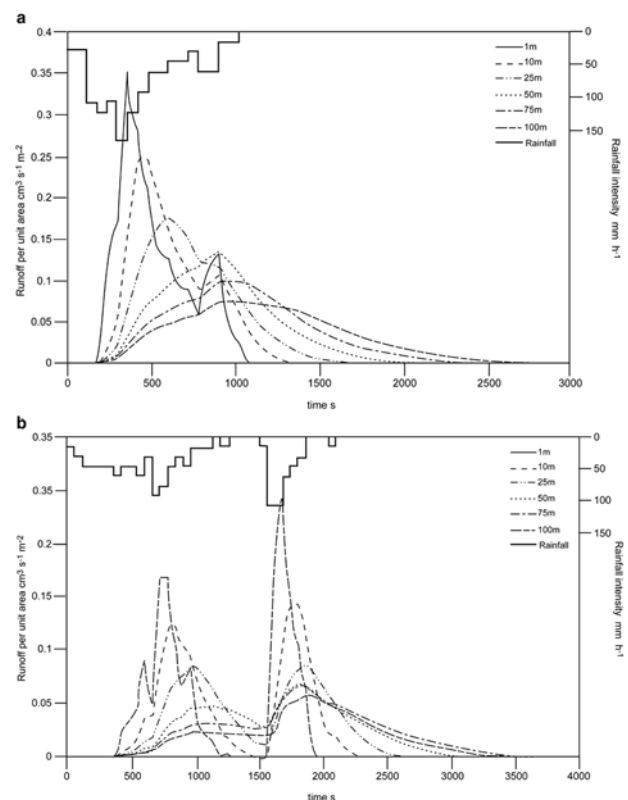


**Figure 2.** Plots of runoff per unit slope area at various points down the hillslope showing the progressive effect of run-on infiltration on the hydrographs: (a) storm 3, showing the effects of a relatively high intensity storm with a single dominant peak; and (b) storm 5, illustrating the effects of a multi-peaked storm. Results are for a  $5^\circ$  slope using infiltration parameters  $a' = 8.6 \text{ mm h}^{-1}$  and  $s_{\text{max}} = 5.8 \text{ mm}$ , and  $ff = 20$ .

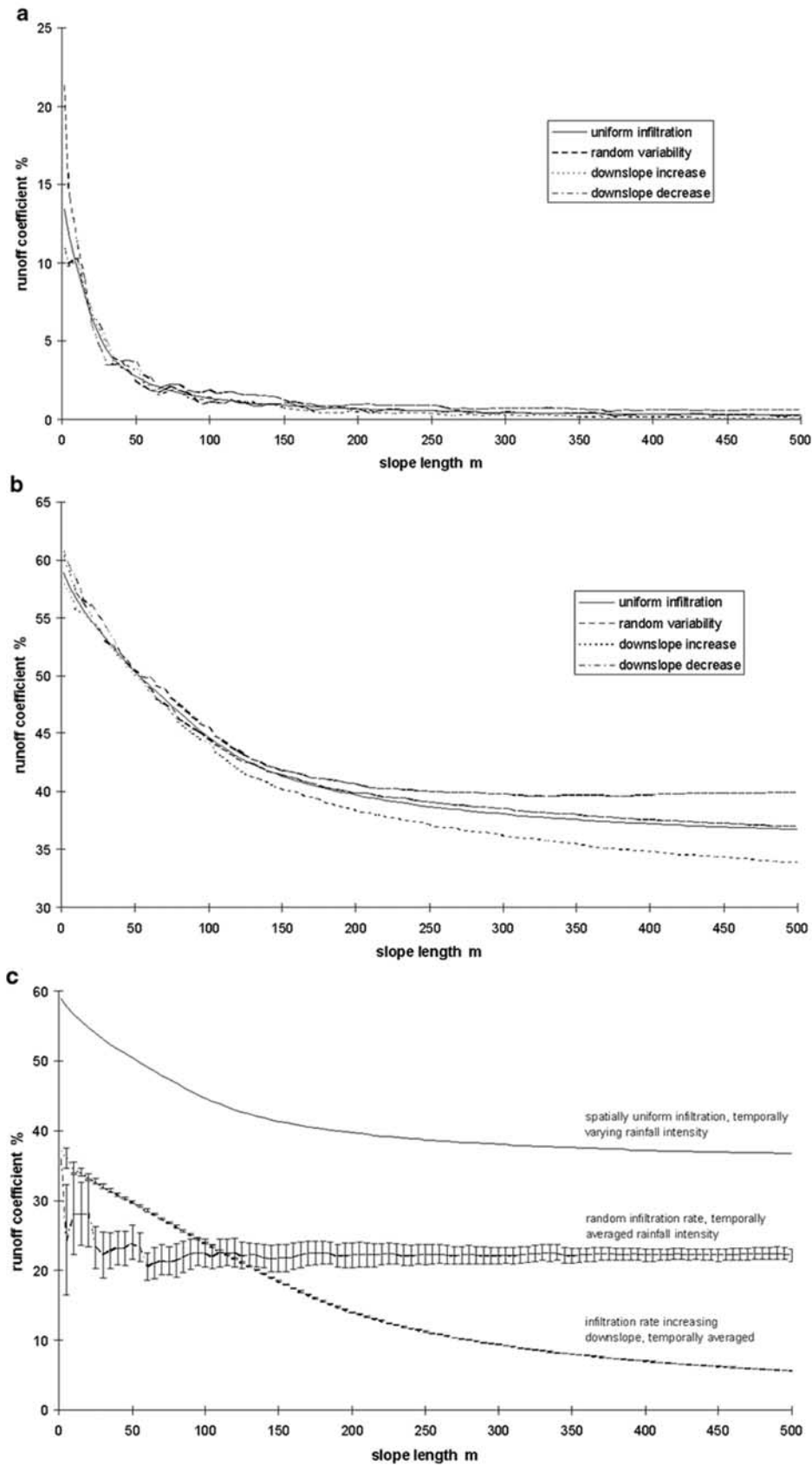


**Figure 3.** Model sensitivity to spatial variability in infiltration parameters on a 5° slope with  $ff=20$ : (a) a storm with a low average intensity (storm 1); (b) a storm with a high average intensity (storm 3); and (c) comparison of the effects of spatial variation in infiltration with the effects of temporal variability in rainfall intensity for storm 3 (bars represent standard errors of 10 replications).

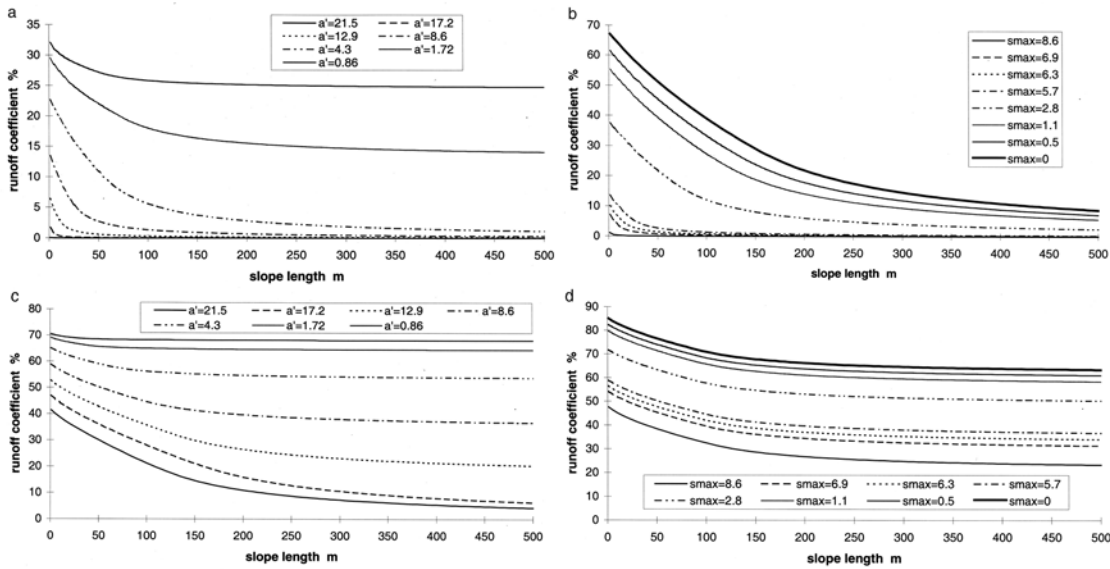


**Figure 4.** Model sensitivity to changes in infiltration parameter for a  $5^\circ$  slope and  $ff = 20$ : (a and b) a storm with a low average intensity (storm 1); and (c and d) a storm with a high average intensity (storm 3). Values of  $a'$  are in  $\text{mm h}^{-1}$ , and values of  $s_{\text{max}}$  are in mm.

seen in the case with uniform infiltration rates (Figure 3). There appear to be no cumulative effects of either positive or negative deviations in any of the storms, so that the pattern observed is simply that of the general trend, but with noise superimposed. Following from this, it is not surprising that the experiments with a downslope increase in infiltration rate produce an even more accentuated decrease in the runoff coefficient with slope length. The reverse was also found to be the case for a downslope decrease in the infiltration rate, although in none of the storms for the initial values of  $a'$  and  $s_{\text{max}}$  did this decrease come close to countering the effect caused by the run-on infiltration.

[14] If the infiltration rates are allowed to vary spatially while maintaining a constant rainfall rate, then there can be an effect of reduced runoff coefficients with increasing slope length, albeit masked by a significant amount of noise (Figure 3c). In the case of storm 3, there was a gradual decrease in runoff coefficients up to a slope length of 75 m, after which the mean value remains about constant. In both cases, the runoff coefficient at a slope length of 500 m was about 62% of that for a length of 1 m. Only in the case where there is a continuous downslope increase in infiltration rates does the spatial pattern of infiltration have a greater relative effect than the temporal variability in the rainfall. Therefore it can be seen that although both explanatory factors are important, the temporal variability of rainfall intensity is by far the more important for most of the sets of conditions investigated.

#### 4. Sensitivity Analysis

[15] Given the importance of temporal variability on the scale-dependency of runoff coefficients, it is useful to test the sensitivity of this control to the variability of other parameters. Thus two further sets of numerical experiments were carried out. First, the sensitivity of the scale dependence in the runoff coefficient to different values of the infiltration parameters was assessed. Second, if the runoff coefficient is affected by slope length because of the

existence of run-on infiltration, then it should also be a function of the flow hydraulics. This linkage occurs because the flow hydraulics affect the available depth of water at any point on the slope and thus control the supply of water available for loss to run-on infiltration. To test this hypothesis, the sensitivity of the runoff coefficient to slope and friction factor was assessed.

##### 4.1. Sensitivity to Infiltration Parameters

[16] The values of the  $a'$  parameter were varied around the initial value of  $8.6 \text{ mm h}^{-1}$ , using multiples of 250, 200, 150, 50, 20, and 10% of the initial value (i.e., 21.5, 17.2, 12.9, 4.3, 1.72, and  $0.86 \text{ mm h}^{-1}$ ), while holding the  $s_{\text{max}}$  parameter constant at its initial value of 5.76 mm. Sensitivity to the  $s_{\text{max}}$  parameter was evaluated in the same way using multiples of 150, 120, 110, 100, 50, 20, and 10% of the initial value (i.e., 8.64, 6.91, 6.33, 5.76, 2.88, 1.15, and 0.58 mm) while holding the value of  $a'$  constant at its initial value. A final parameter set was applied with  $a'$  equal to its initial value and  $s_{\text{max}}$  set to zero, to simulate the effect of rain falling on an already saturated surface. In all cases, the infiltration parameters were the same for each cell in the model.

[17] Higher values of both the  $a'$  and  $s_{\text{max}}$  parameters led to a more marked scale dependency in runoff coefficient in the downslope direction, because these conditions accentuate the amount of run-on infiltration that occurs (Figure 4). Surfaces with a low final infiltration rate are the least sensitive to slope length for the same reason. However, in storms 3 and 5, there is very little change in the runoff coefficient, with  $a' = 0.86 \text{ mm h}^{-1}$ ; the runoff coefficient with a 500-m slope length is still 96.6% of the value for a 1-m slope in storm 3, and 97.2% for storm 5. These results are probably related to the fact that storms 3 and 5 have the highest average intensities in relation to the infiltration rates used.

##### 4.2. Sensitivity to Flow Hydraulics

[18] An initial value for the Darcy-Weisbach friction factor ( $ff$ ) was chosen as 20 (again, a value chosen based

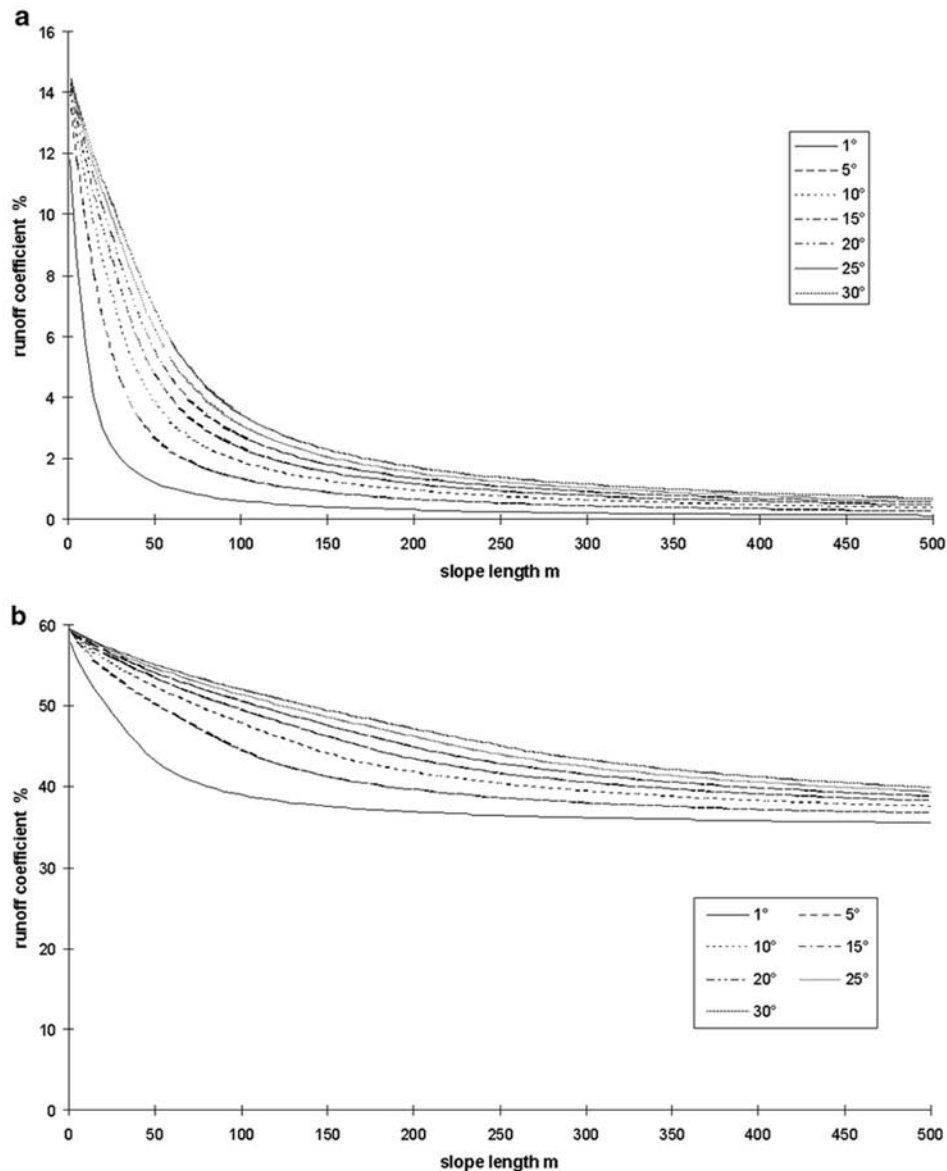


**Figure 5.** Model sensitivity to changes in slope angle using infiltration parameters  $a' = 8.6 \text{ mm h}^{-1}$  and  $s_{\text{max}} = 5.8 \text{ mm}$ , and  $ff = 20$ : (a) a storm with a low average intensity (storm 1); and (b) a storm with a high average intensity (storm 3).

on field measurements [Parsons *et al.*, 1994]), and the slope angle was then varied using values of  $1^\circ$ ,  $5^\circ$ ,  $10^\circ$ ,  $15^\circ$ ,  $20^\circ$ ,  $25^\circ$ , and  $30^\circ$ . The slope angle was then held constant while varying  $ff$  over a range of values (2, 2.5, 5, 10, 20, 40, 80, 120, and 200) consistent with those measured in the field [Parsons *et al.*, 1994].

[19] The sensitivity to flow hydraulics controlled by variations in slope between  $1^\circ$  and  $30^\circ$  is less marked than the range noted for the variations in the infiltration parameters (Figure 5), but there are still important variations according to the slope angle. Higher angles cause the decline in the runoff coefficient to be less rapid with slope length because the runoff is traveling faster and thus has a shorter residence time on the slope and is thus shallower than is the case for lower slope angles. For example, using the initial infiltration and friction factor values in storm 1,

whereas on a  $1^\circ$  slope the change in runoff coefficient for a 1-m slope to a 50-m slope is from 11.8 to 1.2%, the change on a  $30^\circ$  slope is from 14.4 to 6.9%. There is a similar range of variability for values of the friction factor between 2 and 200 (Figure 6). For a 20-m-long,  $5^\circ$  slope the runoff coefficient is 11.8% for  $ff = 2$  and 2.1% for  $ff = 200$  in storm 1. At higher slope angles, the range of values is simply shifted upward: For a 20-m-long,  $30^\circ$  slope the runoff coefficient varies from 13.7% for  $ff = 2$  to 5.4% for  $ff = 200$ . There is thus a positive relationship between the friction factor and the amount of run-on loss, because higher friction factors provide greater depths of slower flow for the same discharge, and thus more water is available for run-on infiltration.

[20] Previous studies [Abrahams and Parsons, 1991b; Abrahams *et al.*, 1994; Wainwright, 1996a, 1996b] have

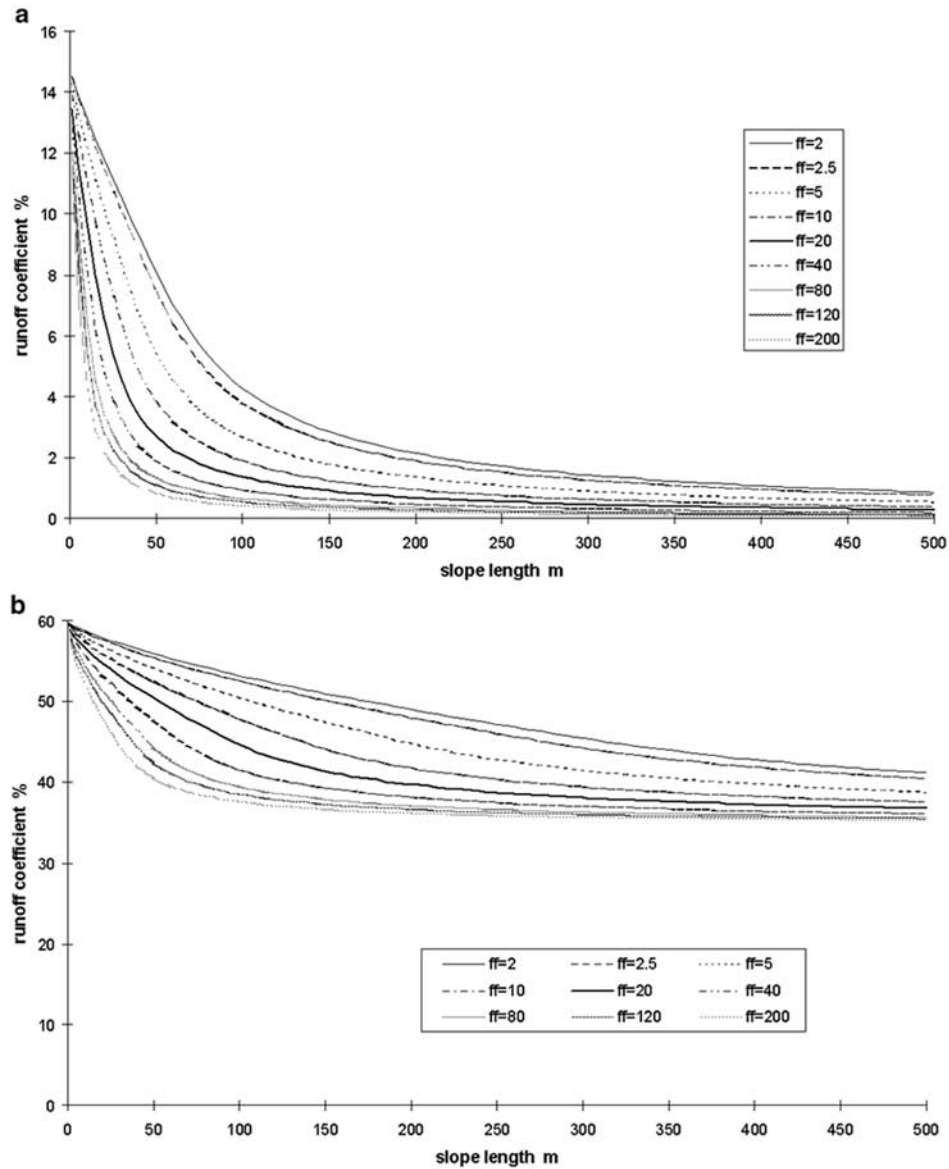


**Figure 6.** Model sensitivity to changes in friction factor on a  $5^\circ$  slope using infiltration parameters  $a' = 8.6 \text{ mm h}^{-1}$  and  $s_{\text{max}} = 5.8 \text{ mm}$ : (a) a storm with a low average intensity (storm 1); and (b) a storm with a high average intensity (storm 3).

demonstrated that there is often a feedback between the flow depth or discharge and the friction factor, as flows become more hydraulically efficient with greater depths. This effect would tend to reduce the amount of run-on loss as flows became more established, and thus reduce the difference in runoff coefficients between longer slopes and shorter ones. To examine the importance of this feedback, a simple model was used of the form

$$ff = 20 - 20d, \quad (4)$$

where  $d$  is the depth of flow [cm]. Note that this is a much more rapid feedback than that measured on desert shrub lands by *Abrahams and Parsons* [1991b] (see the modeling study given by *Scoging et al.* [1992]) because the one-

dimensional study presented here does not permit down-slope accumulation of flow depth from lateral sources.

[21] As expected, this feedback does cause a reduction in the runoff scale dependency, although this reduction is not enough to counter the trend described previously. Using the initial values of the infiltration parameters and a  $1^\circ$  slope, the maximum differences between the results with and without feedback are  $-5.7\%$  in storm 1,  $-1.2\%$  in storm 2,  $-5.4\%$  in storm 3,  $-3.5\%$  in storm 4, and  $-7.3\%$  in storm 5. For a  $30^\circ$  slope, the differences are very similar ( $-5.7\%$ ,  $-0.9\%$ ,  $-4.9\%$ ,  $-3.5\%$  and  $-7.1\%$ , respectively). For storms 1, 2, and 4, there is an asymptotic decrease to this value within the first 20 m of the slope length for the  $1^\circ$  slope and the first 60 m for the  $30^\circ$  slope (Figure 5). For storms 3 and 5 the peak difference occurs further downslope, around 60 m for the  $1^\circ$  slope and between 300 and 350 m for the  $30^\circ$  slope, and is



followed by a subsequent reduction in the difference. These differences are most likely to be due to the different slope lengths at which equilibrium runoff is reached.

## 5. Conclusions

[22] The numerical experiments described in this paper demonstrate that temporal variability in rainfall is a significant factor in controlling the scale-dependency of runoff coefficients. Run-on infiltration of water produced during pulses of high-intensity rainfall as it moves downslope is suggested to be the mechanism by which this scale dependency occurs. These results are independent of the specific infiltration model used, as similar results were also produced by adapting the *Smith and Parlange* [1978] infiltration model to account for run-on infiltration in a small number of replications. Sensitivity analysis indicates that the scale dependency of the runoff coefficient is most sensitive to the values of the infiltration parameters and their relative magnitudes compared to the rainfall characteristics. Flow hydraulics are also significant and are affected to an equal degree by the slope angle and the friction factor. In the latter case, conditions with greater mean flow depths, i.e., where there are less steep slopes and/or rougher surfaces, will cause the observed effect to be greater. Neither observed feedbacks between friction factor and flow depth nor spatial patterns in the infiltration rates were of a sufficient magnitude to counter the effects produced by the run-on infiltration. These results are significant in providing an alternative explanation for the scale dependency in runoff coefficients.

[23] The results of this study are also important in that they provide insight into some of the minimum requirements for models of overland flow and their parameterization. If rainfall rates are not allowed to vary through time, then flow events will be commonly underpredicted where run-on infiltration accounts for the progressive loss of water downslope. The extent of the underprediction increases with the length of the slope being simulated. In the case where the mean infiltration rates are close to the mean rainfall intensity, overland-flow events may be missed completely. These results suggest that where a model is sensitive to the amount of flow produced, it should be parameterized with high-resolution rainfall data, preferably at bucket-tip resolution. Where this is not possible, stochastic rainfall models that replicate persistence in intensities through a storm [e.g., *Charles et al.*, 1999; *Cowperton and O'Connell*, 1997] are likely to be preferable to the assumption of uniform intensity rainfall. The temporal resolution of rainfall required for any particular setting will depend on the length of slope, as illustrated by the feedbacks demonstrated with the flow hydraulics. Preferably, the resolution should be better than the time required for the flow to traverse a model cell. Where monitored data from plots are used to provide parameters for overland-flow models, it is likely that errors will be produced if the scale-dependency discussed here is not taken into account. Model parameterization should thus be carried out at an equivalent scale to that of the model grid size (see *Parsons et al.* [1997] for a further illustration of this).

[24] **Acknowledgments.** We gratefully acknowledge the rainfall data provided by NOAA, which were supplied by John Ensworth. The rainfall data from Jornada were collected as part of the Jornada Long-Term

Ecological Research (LTER) Program funded by the U.S. National Science Foundation (grant DEB 94-11971). We thank John Anderson for his assistance in collecting these data. We would like to thank Mike Kirkby and two anonymous referees for making invaluable comments on an earlier version of this paper. Roma Beaumont assisted in the drawing of Figure 2.

## References

- Abrahams, A. D., and A. J. Parsons, Relation between infiltration and stone cover on a semiarid hillslope, southern Arizona, *J. Hydrol.*, 122, 49–59, 1991a.
- Abrahams, A. D., and A. J. Parsons, Resistance to overland flow on desert pavement and its implications for sediment transport modelling, *Water Resour. Res.*, 27, 1827–1836, 1991b.
- Abrahams, A. D., A. J. Parsons, and J. Wainwright, Resistance to overland flow on semiarid grassland and shrubland hillslopes, Walnut Gulch, southern Arizona, *J. Hydrol.*, 156, 431–446, 1994.
- Artan, G. A., C. M. U. Neale, and D. G. Tarboton, Characteristic length scale of input data in distributed models: implications for modelling grid size, *J. Hydrol.*, 227, 128–139, 2000.
- Charles, S. P., B. C. Bates, and J. P. Hughes, A spatio-temporal model for downscaling precipitation occurrence and amounts, *J. Geophys. Res.*, 104, 31,657–31,669, 1999.
- Corradini, C., F. Melone, and R. E. Smith, A unified model for infiltration and redistribution during complex rainfall patterns, *J. Hydrol.*, 192, 104–124, 1997.
- Cowperton, P. S. P., and P. E. O'Connell, A regionalised Neyman-Scott model of rainfall with convective and stratiform cells, *Hydrol. Earth Syst. Sci.*, 1, 71–80, 1997.
- Dubreuil, P. L., Review of field observations of runoff generation in the tropics, *J. Hydrol.*, 80, 237–264, 1985.
- Dunne, T., W. Zhang, and B. F. Aubry, Effects of rainfall, vegetation, and microtopography on infiltration and runoff, *Water Resour. Res.*, 27, 2271–2285, 1991.
- Faurès, J.-M., D. C. Goodrich, D. A. Woolhiser, and S. Sorooshian, Impact of small-scale spatial rainfall variability on runoff modelling, *J. Hydrol.*, 173, 309–326, 1995.
- Hawkins, R. H., Interpretations of source-area variability in rainfall-runoff relations, in *Rainfall-Runoff Relationship*, pp. 303–323, Water Resour. Publ., Littleton, Colo., 1982.
- Julien, P. Y., and G. E. Moglen, Similarity and length scale for spatially varied overland flow, *Water Resour. Res.*, 26, 1819–1832, 1990.
- Kirkby, M. J., Modelling water erosion processes, in *Soil Erosion*, edited by M. J. Kirkby and R. P. C. Morgan, pp. 183–216, John Wiley, New York, 1978.
- Lal, R., Soil degradative effects of slope length and tillage methods on alfisols in Western Nigeria, I, Runoff, erosion and crop response, *Land Degradation Dev.*, 8(3), 201–219, 1997.
- Larsen, J. E., M. Sivapalan, N. A. Coles, and P. E. Linnet, Similarity analysis of runoff generation in real-world catchments, *Water Resour. Res.*, 30, 1641–1652, 1994.
- Merz, B., and A. Bárdossy, Effects of spatial variability on the rainfall runoff process in a small loess catchment, *J. Hydrol.*, 212–213, 304–317, 1998.
- Merzougi, M., and G. F. Gifford, Spatial variability of infiltration rates on a semiarid seeded rangeland, *Hydrol. Sci. J.*, 32, 243–250, 1987.
- Parsons, A. J., A. D. Abrahams, and J. Wainwright, On determining resistance to interrill overland flow, *Water Resour. Res.*, 30, 3515–3521, 1994.
- Parsons, A. J., J. Wainwright, A. D. Abrahams, and J. R. Simanton, Distributed dynamic modelling of interrill overland flow, *Hydrol. Processes*, 11(14), 1833–1859, 1997.
- Scoging, H., Modelling overland-flow hydrology for dynamic hydraulics, in *Overland Flow: Hydraulics and Erosion Mechanics*, edited by A. J. Parsons and A. D. Abrahams, pp. 89–103, UCL Press, London, 1992.
- Scoging, H., A. J. Parsons, and A. D. Abrahams, Application of a dynamic overland-flow hydraulic model to a semi-arid hillslope, Walnut Gulch, Arizona, in *Overland Flow: Hydraulics and Erosion Mechanics*, edited by A. J. Parsons and A. D. Abrahams, pp. 105–145, UCL Press, London, 1992.
- Sharma, M. L., G. A. Gander, and C. G. Hunt, Spatial variability of infiltration in a watershed, *J. Hydrol.*, 45, 101–122, 1980.
- Sivapalan, M., and E. F. Wood, Spatial heterogeneity and scale in the infiltration response of catchments, in *Scale Problems in Hydrology: Runoff Generation and Basin Response*, edited by V. K. Gupta,

- I. Rodríguez-Iturbe, and E. F. Wood, pp. 81–106, D. Reidel, Norwell, Mass., 1986.
- Smith, R. E., and J.-Y. Parlange, A parameter-efficient hydrologic infiltration model, *Water Resour. Res.*, *14*, 533–538, 1978.
- Thornes, J. B., and A. Gilman, Potential and actual erosion around archaeological sites in Spain, in *Rainfall Simulation, Runoff and Soil Erosion*, edited by J. de Ploey, *Catena Suppl.*, *4*, 91–114, 1984.
- Van de Giesen, N. C., T. J. Stomph, and N. DeRidder, Scale effects of Hortonian overland flow and rainfall-runoff dynamics in a West African catena landscape, *Hydrol. Processes*, *14*, 165–175, 2000.
- Van Loon, E. E., and K. J. Keesman, Identifying scale-dependent models: The case of overland flow at the hillslope scale, *Water Resour. Res.*, *36*, 243–254, 2000.
- Wainwright, J., Infiltration, runoff and erosion characteristics of agricultural land in extreme storm events, SE France, *Catena*, *26*, 27–47, 1996a.
- Wainwright, J., A comparison of the interrill infiltration, runoff and erosion characteristics of two contrasting “badland” areas in southern France, *Z. Geomorphol. Suppl.*, *106*, 183–198, 1996b.
- Wainwright, J., Climate and climatological variations, in *Structure and Function of a Chihuahuan Desert Ecosystem: The Jornada LTER*, edited by W. H. Schlesinger, K. M. Havstad, and L. F. Huenneke, Oxford Univ. Press, New York, in press, 2002.
- Wainwright, J., M. Mulligan, and J. B. Thornes, Plants and water in drylands, in *Ecohydrology*, edited by A. J. Baird and R. L. Wilby, pp. 78–126, Routledge, New York, 1999.
- Wilcox, B. P., B. D. Newman, D. Brandes, D. W. Davenport, and K. Reid, Runoff from a semiarid ponderosa pine hillslope in New Mexico, *Water Resour. Res.*, *33*, 2301–2314, 1997.
- Williams, J., and M. Bonell, The influence of scale of measurement on the spatial and temporal variability of the Philip infiltration parameters—An experimental study in an Australian savannah woodland, *J. Hydrol.*, *104*, 33–51, 1988.
- Yair, A., and A. Kossovsky, Climate and surface properties: Hydrological response of small and semi-arid watersheds, *Geomorphology*, *42*, 43–57, 2002.
- Yair, A., and H. Lavee, Runoff generation in arid and semi-arid zones, in *Hydrological Forecasting*, edited by M. G. Anderson and T. P. Burt, pp. 183–220, John Wiley, New York, 1985.
- Yair, A., D. Sharon, and H. Lavee, Trends in runoff and erosion processes over an arid limestone hillside, northern Negev, Israel, *Hydrol. Sci. Bull.*, *25*, 243–255, 1980.
- Zhu, T. X., L. E. Band, and R. A. Vertessy, Continuous modelling of intermittent stormflows on a semi-arid agricultural catchment, *J. Hydrol.*, *226*, 11–29, 1999.

---

A. J. Parsons, Department of Geography, Leicester University, University Road, Leicester, LE1 7RH, UK.

J. Wainwright, Department of Geography, King's College London, Strand, London, WC2R 2LS, UK. (john.wainwright@kcl.ac.uk)